^{18}F Choline PET/CT in the Preoperative Staging of Prostate Cancer in Patients with Intermediate or High Risk of Extracapsular Disease: A Prospective Study of 130 Patients[1]

Mohsen Beheshti, MD
Larisa Imamovic, MD
Gabriele Broinger, MD
Reza Vali, MD
Peter Waldenberger, MD
Franz Stoiber, MD
Michael Nader, PhD
Bernhard Gruy, MS
Guenter Janetschek, MD
Werner Langsteger, MD

Purpose: To prospectively evaluate the potential value of fluorocholine (FCH) positron emission tomography (PET)/computed tomography (CT) in the preoperative staging of patients with prostate cancer who had intermediate or high risk of extracapsular disease.

Materials and Methods: Institutional review board approval and written informed consent were obtained. Overall, 132 patients with prostate cancer (mean age, 63 years ± 7 [standard deviation]) were enrolled between October 2003 and June 2008. Two patients were subsequently excluded. In 111 patients, radical prostatectomy with extended pelvic lymph node (LN) dissection was performed. Patients were categorized into groups with intermediate (n = 47) or high (n = 83) risk of extracapsular extension on the basis of their Gleason scores and prostate specific antigen levels. Imaging was performed with an integrated PET/CT system after injection of 4.07 MBq FCH per kilogram of body weight with acquisition of dynamic images in the pelvis and whole-body images. Statistical analysis was performed on a per-patient basis.

Results: Significant correlation was found between sections with the highest FCH uptake and sextants with maximal tumor infiltration (r = 0.68; P = .0001). Overall, 912 LNs were histopathologically examined. A per-patient analysis revealed the sensitivity, specificity, and positive and negative predictive values of FCH PET/CT in the detection of malignant LNs were 45%, 96%, 82%, and 83%, respectively. For LN metastases greater than or equal to 5 mm in diameter, sensitivity, specificity, and positive and negative predictive values were 66%, 96%, 82%, and 92%, respectively. In 13 patients, 43 bone metastases were detected. Early bone marrow infiltration was detected with only FCH PET in two patients. FCH PET/CT led to a change in therapy in 15% of all patients and 20% of high-risk patients.

Conclusion: FCH PET/CT could be useful in the evaluation of patients with prostate cancer who are at high risk for extracapsular disease, and it could be used to preoperatively exclude distant metastases.

Supplemental material: *http://radiology.rsna.org/lookup/suppl/doi:10.1148/radiol.09090413/-/DC1*

[1] From the Department of Nuclear Medicine and Endocrinology, PET-CT Center Linz (M.B., L.I., R.V., M.N., B.G., W.L.), St Vincent's Hospital, Seilerstaette 4, A-4020 Linz, Austria; Departments of Clinical Pathology (G.B.), Radiology (P.W.), and Urology (F.S.), St Vincent's Hospital, Linz, Austria; and Department of Urology, Elisabethinen Hospital, Linz, Austria (G.J.). Received March 11, 2009; revision requested April 9; revision received August 4; accepted September 18; final version accepted October 20. **Address correspondence to** M.B. (e-mail: *mohsen.beheshti@bhs.at*).

Prostate, lung, and colorectal cancers account for more than 56% of all newly diagnosed cancers in men (1). In Western Europe and North America, prostate cancer is the most common malignancy in men, and it accounts for about 33% (n = 232 090) of incident cases in the United States (1,2).

The accurate detection of disease confined to the prostate gland versus extraglandular spread to the lymph nodes (LNs) or skeleton is of key importance when defining the therapeutic approach. Imaging modalities play an important role in the staging of prostate cancer. However, the optimal use of imaging modalities in the staging of prostate cancer is still under debate, as the reported sensitivity and specificity of current imaging methods—such as bone scintigraphy, computed tomography (CT), magnetic resonance (MR) imaging, and ultrasonography (US)—vary considerably (3,4).

Positron emission tomography (PET) is a promising modality for use in metabolic tumor imaging. Fluorine 18 (^{18}F) fluorodeoxyglucose (FDG) PET is effective in the detection of primary lesions and metastases in a number of different tumor types. However, the results in patients with prostate cancer have been somewhat disappointing and inconsistent (5–10). Low FDG avidity of most prostate cancer cells and urinary activity are suggested as the main limitations of ^{18}F FDG PET in the evaluation of patients with prostate cancer (5).

Relatively recently, carbon 11 (^{11}C)- or ^{18}F-labeled choline PET has been used in the assessment of patients with prostate cancer (11–16). However, the value of PET with radiolabeled choline in the staging of prostate cancer has been a subject of controversy, and varying results have been reported (4,11,16–19).

The purpose of this study was to prospectively evaluate the potential value of fluorocholine (FCH) PET/CT in the preoperative staging of patients with prostate cancer who had intermediate or high risk of extracapsular disease.

Advances in Knowledge

- Fluorocholine (FCH) PET/CT enabled the detection of 43 metastatic bone lesions in one intermediate-risk and 12 high-risk patients with prostate cancer; only FCH PET was able to depict bone metastases, probably because of early marrow-based bony involvement in two of 13 patients.
- FCH PET/CT has limited value in the detection of malignant lymph nodes, especially lymph nodes smaller than 5 mm in diameter.
- A significant correlation (r = 0.68, P = .0001) was found between regions with maximal FCH uptake on PET/CT images and sextants with maximum tumor involvement at histopathologic analysis.

Materials and Methods

Patients

This study was approved by the ethical committee of St Vincent's Hospital, and written informed consent was obtained from all patients. A total of 132 consecutive men (mean age, 63 years ± 7 [standard deviation]) with biopsy-proved prostate cancer who were scheduled to undergo surgery were enrolled in this prospective study between October 1, 2003, and June 1, 2008. Only patients with a Gleason summed score of at least seven and/or a prostate specific antigen (PSA) level greater than 10 ng/mL (10 μg/L) were included. The exclusion criteria were a second cancer and neoadjuvant hormonal or radiation therapy prior to surgery. Two patients with prostatitis were subsequently excluded from the study because there was a discrepancy between the preoperative biopsy findings and the final histopathologic results; this was similar to the findings in a previous study that were reported as "vanishing cancer phenomenon" (20). All patients underwent ^{18}F FCH PET/CT at least 14 days after US-guided biopsies to avoid any biopsy effect. Free PSA serum concentration was determined on the day of FCH PET/CT (mean, 27 ng/mL ± 49 [27 μg/L ± 49]; range, 0.25–462 ng/mL [0.25–462 μg/L]). The mean Gleason summed score defined at biopsy was 7.4 (range, four to 10).

Patients were categorized into two groups: those with intermediate risk of extracapsular tumor (n = 47) (PSA level, 10–20 ng/mL [10–20 μg/L]; Gleason score, seven) and those with high risk of extracapsular tumor (n = 83) (PSA level >20 ng/mL [>20 g/μL], Gleason score of at least eight).

Only patients with clinical organ-confined tumor stages and a life expectancy of at least 10 years underwent open retropubic radical prostatectomy with extended pelvic LN dissection (removal of obturator, external iliac, and internal iliac LNs with or without presacral and common iliac LNs).

Implication for Patient Care

- FCH PET/CT led to changes in the therapeutic care of 20% of patients with prostate cancer who were at high risk for extracapsular disease, suggesting that this modality will be helpful in the triage of this cohort.

Published online
10.1148/radiol.09090413

Radiology 2010; 254:925–933

Abbreviations:
FCH = fluorocholine
FDG = fluorodeoxyglucose
LN = lymph node
PSA = prostate specific antigen
SUV_{max} = maximum standardized uptake value

Author contributions:
Guarantors of integrity of entire study, M.B., R.V., M.N., W.L.; study concepts/study design or data acquisition or data analysis/interpretation, all authors; manuscript drafting or manuscript revision for important intellectual content, all authors; manuscript final version approval, all authors; literature research, M.B., L.I., R.V., M.N., B.G., G.J., W.L.; clinical studies, M.B., G.B., R.V., F.S., M.N., G.J., W.L.; statistical analysis, M.B., R.V., M.N., B.G., W.L.; and manuscript editing, M.B., R.V., P.W., M.N., G.J., W.L.

Authors stated no financial relationship to disclose.

PET/CT Imaging

^{18}F FCH (fluoromethyl-dimethyl-2-hydroxyethyl-ammonium) was synthesized on site (Iasocholine), as described by Vassiliev et al (21). Imaging was performed with an integrated PET/CT system (Discovery LS; GE Medical Systems, Milwaukee, Wis) that consisted of a full-ring PET scanner with a 14.6-cm transverse field of view and an in-plane resolution of 4.8 mm full width at half maximum at the center of the field of view and a four-section CT scanner. All PET images were acquired with the two-dimensional mode (4 minutes emission per bed position) and were reconstructed with standard reconstruction ordered-subset expectation maximization iterative algorithm (two iterative steps) and were reformatted into transverse, coronal, and sagittal views. As a routine protocol, imaging started 1 minute after intravenous injection of FCH (4.07 MBq per kilogram of body weight), with acquisition of dynamic PET images at one constant bed position of the pelvic region (covering the pelvic floor and urinary bladder) for 8 minutes (1 minute per frame) to overcome the effect of urinary activity in the bladder.

Six- or seven-bed-position whole-body images were acquired with an acquisition time of 4 minutes per bed position from the thigh to the base of the skull 10 minutes after injection. The number of images acquired depended on the size of the patient. In case of abnormal FCH accumulation in the whole-body images, a delayed static acquisition was performed over the abnormal tracer uptake 90–120 minutes after injection.

Unenhanced CT was performed for localization and attenuation correction (140 kV, 0.5 second per rotation, 5.0-mm reconstructed section thickness, 0.5-mm overlap) with a low-beam current modulation (80–120 mA). In patients with positive FCH lesions, an additional contrast material–enhanced (100 mL of iodixanol, 270 mg of iodine per milliliter, Visipaque; GE Healthcare, Cork, Ireland) CT study of the pelvis, abdomen, or both was performed with high-beam tube current modulation (120–330 mA; 0.5 second per rotation; 5.0-mm reconstructed section thickness; 0.5-mm overlap; 512 × 512 matrix; pitch index, 1.5) based on the angular modulation technique (SmartScan; GE Medical Systems, Waukesha, Wis), which automatically adjusts the tube current for each projection angle to the attenuation of the patient to minimize x-rays in projection angles that are less important with regard to reducing the overall noise content. The reformatted, transverse, coronal, and sagittal views were used for interpretation.

Image Interpretation and Data Analysis

PET images were interpreted by two nuclear medicine specialists (M.B., W.L.; 5 and 10 years of experience, respectively) who were aware of the referral diagnosis and risk assessment of extracapsular disease. They had access to the CT and PET/CT images for morphologic correlation and localization of abnormal PET lesions. Images were read sequentially within a maximum of 3 days after the performance of each study by using advanced PET/CT review software (Advantage for Windows, versions 4.2 through 7; GE Medical Systems), which allows simultaneous scrolling through the corresponding PET, CT, and fusion images in transverse, coronal and sagittal planes.

A lesion was considered abnormal when focal tracer accumulation was greater than background activity. Semiquantitative analysis of the abnormal radiotracer uptake was performed by using the maximum standardized uptake value (SUV_{max}). To determine the SUV_{max}, a volume of interest covering the entire abnormal lesion was drawn (M.B., W.L.). The average value of the five voxels with the highest activity was calculated to minimize overestimation of the SUV_{max} caused by a single high-activity voxel. SUV_{max} was also measured in the first and last frames of dynamic PET images.

The diagnosis of malignant LNs on PET images was based on the visual assessment of focal increased FCH uptake corresponding to LN chains on CT images. At PET imaging, LNs with increased tracer uptake were considered positive for metastatic spread, even if their short-axis diameter was less than 10 mm. LNs without abnormal tracer uptake were considered benign on PET images, even if their short-axis diameter was larger than 10 mm.

The CT data were interpreted by a radiologist (P.W., 15 years experience) who was aware of only the referral diagnosis. LNs were categorized as malignant on CT images because the short-axis diameter was larger than 10 mm, contrast enhancement was visible, and there was neither fatty hilus nor round configuration. Whether bone lesions were considered malignant depended on their anatomic location (posterior aspect of the vertebral body and pedicle), characteristic morphologic changes (cortical destruction), or both. Discrete FCH uptake in only inguinal LNs was interpreted as possible reactive uptake (12,15); therefore, it was excluded from data analysis. The final interpretations were made by two nuclear medicine specialists (M.B., W.L.) and a board-certified radiologist (P.W.) working in consensus.

Histopathologic Correlation and Assessment of Additional Findings

Patients who had no evidence of LNs or bone metastases at FCH PET/CT (n = 111) underwent radical prostatectomy and extended pelvic LN dissection 24.2 days ± 7.5 (median, 22 days; range, 2–38 days) after FCH PET/CT. Visualized prostate volume on PET images was cut by means of the aforementioned commercially available software program. On the basis of a sextant biopsy template, the extrapolated prostate volume was divided equally into basal, middle, and apical thirds on each side. The segment with the highest tracer intensity was identified and visually compared with the sextant with maximum tumor involvement at histopathologic examination. The surgically resected specimens were fixed in formalin. After fixation, the prostate specimens were then step-sectioned at 0.5-cm intervals perpendicular to the long axis from the apex to the base. Histologic samples were obtained from at least two slices of tissue. The paraffin-embedded samples were routinely stained with hematoxylin-eosin.

The exact location and extension of carcinomatous tissue were determined independently by a pathologist (G.B., 6 years experience). Visual comparison of FCH PET/CT findings with histopathologic findings was performed in consensus (M.B., W.L., G.B.).

In patients who underwent lymphadenectomy, PET/CT findings were correlated with histopathologic results. Postoperative histopathologic evaluation of LNs consisted of a standard protocol of step sections in 250-μm sequences (conventional hematoxylin-eosin staining) and immunohistochemistry of each step, respectively. The malignant LNs were categorized into three groups on the basis of tumor diameter: those 2 mm or smaller (micrometastases), those larger than 2 mm but smaller than 5 mm, and those 5 mm or larger.

Patients with evidence of LNs, bone metastases, or both at FCH PET/CT were not considered for surgery and therefore underwent nonoperative therapeutic procedures (neoadjuvant hormonal or radiation therapy). Follow-up FCH PET/CT was performed in these patients after 6 months (range, 6–24 months).

Final Diagnosis

LN staging.—The final diagnosis of positive LNs on PET images was based on histopathologic findings in 25 patients and on the results of follow-up imaging studies (FCH PET/CT) in 15 patients, none of whom underwent surgery. Lesions with increased FCH uptake were considered malignant at follow-up studies if they showed persistent or increased FCH uptake with corresponding pathologic morphologic changes on CT images or if decreased FCH activity with clinically regressive findings was seen after treatment.

Bone metastases staging.—The bone lesions were considered malignant if they were positive at both FCH PET and CT, with corresponding positive uptake as assessed with a bone-seeking modality (^{18}F PET/CT or bone scanning) or positive MR imaging findings.

If there was a discrepancy between FCH PET and CT findings, it had to be proved to be a metastasis at clinical and FCH PET/CT follow-up examinations for at least 6 months (range, 6–24 months). Lesions with increased FCH uptake on the follow-up PET images with corresponding malignant morphologic changes on CT images and clinical evidence of disease progression were considered malignant.

Statistical Analysis

The sensitivity, specificity, and positive and negative predictive values were calculated by using data collected during PET studies on a per-patient basis. Each patient with at least one PET-positive LN that was finally confirmed to be malignant at histopathology, follow-up imaging, or both was considered to have a true-positive finding. Patients with negative FCH PET findings but positive histopathologic results were considered to have a false-negative finding. Patients with positive FCH accumulation in the pelvic and/or abdominal LNs but negative histopathologic results were considered to have a false-positive finding. Patients with both negative FCH PET and histopathologic results were considered to have a true-negative finding. The Pearson correlation test was used to assess correlations between PSA levels and Gleason scores with the SUV_{max} in the prostate, as well as the correlation between sections with the highest FCH uptake on PET images and sextants with maximal tumoral infiltration at histopathologic analysis. The paired *t* test was used to compare mean SUV_{max} in malignant LNs with that in benign LNs and bone lesions. Statistical software (SPSS, Chicago, Ill) was used for the calculations. $P < .05$ was indicative of a significant difference.

Results

A total of 111 patients underwent radical prostatectomy with extended pelvic LN dissection, while 19 were upstaged because LNs, bone metastases, or both were detected at PET/CT.

Primary Staging

All patients had abnormal increased tracer uptake in the prostate. A significant correlation was found in the whole study group between sections with highest FCH uptake at PET and sextants with maximal tumoral infiltration at histopathologic analysis ($r = 0.68$, $P = .0001$; Fig 1).

The mean SUV_{max} in the prostate was 5.5 (range, 1.6–22.3) in the dynamic images, 6.7 (range, 2.3–26.0) in the whole-body images, and 6.1 (range, 1.7–13.5) in the late images. There was no significant correlation between SUV_{max} in the prostate and PSA levels or Gleason scores ($P = .10$ and $P = .28$, respectively).

LN Staging

Overall, 912 sampled LNs were histopathologically examined (mean number of LNs per patient, eight; median, nine; range, two to 24). Forty (31%) of the 130 patients had 85 malignant LNs that were validated either with histopathologic analysis (25 patients) or follow-up studies (15 patients) (Table E1 [online]). Six of 40 patients belonged to the intermediate-risk group, while 34 belonged to the high-risk group.

In 18 of the 130 patients, FCH PET findings were positive for 47 malignant LNs (true-positive findings). This finding was confirmed at histopathologic analysis in three patients and at follow-up studies in 15 patients. In 22 patients with 38 malignant LNs, FCH PET findings were negative (false-negative findings): Ten of these patients had micrometastases (≤2 mm in diameter), three patients had a tumor diameter of more than 2 mm but less than 5 mm, and nine patients with malignant LNs with a diameter of at least 5 mm. Sixteen of 22 patients with false-negative FCH PET findings had only malignant LNs no larger than 5 mm in diameter.

The average maximum diameter of the malignant LNs detected with FCH PET/CT was 15.6 mm (range, 5.0–30.0 mm; median, 15.0 mm). The mean diameter of the true-positive LNs was significantly larger than that of the false-negative LNs (15.6 mm vs 4.0 mm, $P = .0001$). The mean SUV_{max} of malignant LNs was 9.1 (range, 2.1–33.8; median, 7.0), which generally decreased in the images obtained later in the examination (mean SUV_{max}, 7.7; range, 1.0–19.4; median, 7.2).

Figure 1

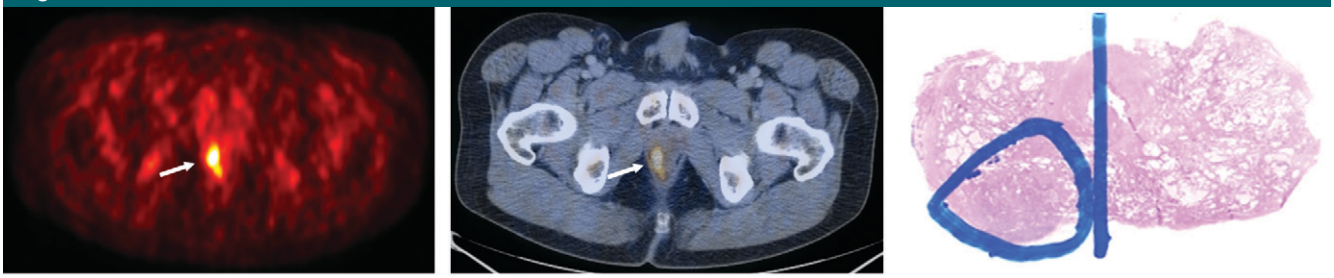

a. b. c.

Figure 1: Images obtained in a 66-year-old man with biopsy-proved prostate cancer (Gleason score, seven; PSA level, 7.8 ng/mL [7.8 μg/L]). **(a)** Transaxial FCH PET image with increased tracer uptake in the prostate (arrow). **(b)** Fusion FCH PET/CT image shows the localization of increased tracer uptake in the right apical part of the prostate (arrow). **(c)** Apical slice of histopathologic sextants of the prostate. The marked region (blue) is the maximum tumor infiltration clearly correlated with abnormal FCH uptake.

In four patients, FCH PET/CT findings were false-positive (one sinus histiocytosis, three reactive LNs). All four LNs showed FCH hyperperfusion on the images obtained early in the examination (1–3 minutes; mean SUV_{max}, 4.85 ± 1.24), followed by rapid washout on the dynamic (8 minutes; SUV_{max}, 2.47 ± 0.73) and delayed (SUV_{max}, 2.09 ± 0.65) semi-whole-body images (Fig 2). In contrast, malignant LNs showed a constant or an increasing pattern of FCH uptake during acquisition of dynamic images with a mean SUV_{max} of 5.90 ± 2.53 (1 minute after injection) and 7.85 ± 3.20 (8 minutes after injection), respectively.

A per-patient analysis showed the sensitivity, specificity, and positive and negative predictive values of FCH PET/CT were 45%, 96%, 82%, and 83%, respectively, in the detection of malignant LNs and 66%, 96%, 82%, and 92%, respectively, in the detection of LN metastases at least 5 mm in diameter (Table 1).

Bone Metastases Staging

A total of 43 metastatic bone lesions were detected in 13 of 130 patients (one intermediate-risk patient and 12 high-risk patients) with FCH PET/CT. The mean SUV_{max} in malignant bone lesions was 9.0 ± 4.0 (range, 3.6–18.3; median, 7.7) on whole-body images and showed significantly increased uptake ($P < .001$) in the delayed images (mean SUV_{max}, 12.2 ± 6.0; range, 3.7–27.0; median, 13.2). Probably as a result of early bone marrow infiltration in two of these 13 patients, only FCH PET findings were positive, without any substantial morphologic changes on CT images (Fig 3).

Clinical Staging and Therapy Management

FCH PET/CT results prompted us to switch from operative therapy to nonoperative therapy in 19 (15%) of 130 patients: We detected retroperitoneal LNs in six patients, metastatic bone disease in four patients, and both LN and bone metastases in nine patients (Fig 4). All but two of these patients were in the high-risk group. When considering the entire high risk group, 17 (20%) of 83 cases were upstaged on the basis of the PET/CT findings. All detected lesions in these patients were proved to be malignant at FCH PET/CT follow-up examinations for at least 6 months (range, 6–24 months).

Discussion

The goal of current cancer care is to administer risk-adjusted patient-specific treatment planned to maximize cancer control while minimizing the risk of complications (4). Therefore, accurate characterization of the tumor and staging of disease is of great importance in choosing the appropriate therapeutic management from a wide array of alternatives, including deferred therapy (watchful waiting), androgen ablation, radical surgery, and external radiation (22). MR imaging and transrectal US are often used to evaluate local tumor stage (T stage), and CT and bone scanning are performed to assess LNs (N stage) and distant metastases (M stage), respectively. However, despite their relatively high sensitivity, conventional morphologic imaging modalities suffer from inadequate specificity, particularly in the detection of LN metastases (3). With the use of lymphotropic superparamagnetic nanoparticles in MR imaging, detection of LN metastases might be improved. In a lesion-based study in which 71.4% of metastatic LNs in patients with prostate cancer were within the normal size range, Harisinghani et al (23) found a sensitivity and specificity of 35.4% and 90.4%, respectively, for conventional MR imaging versus a sensitivity and specificity of 90.5% and 97.8%, respectively, for MR imaging with lymphotropic superparamagnetic nanopaticles.

Reports have emphasized the potential advantages of PET performed with radiotracers such as ^{11}C acetate, ^{11}C- and ^{18}F-labeled fluoroethylcholine, and ^{18}F FCH in the assessment of patients with prostate cancer (10,12–14).

Two possible mechanisms have been suggested to explain the increased choline uptake in prostate cancer cells (5,24). The first is increased cell proliferation in tumors. Choline is a precursor for the biosynthesis of phosphatidylcholine and other phospholipids that are the major components of cell membrane. It seems that choline uptake is a marker of cell proliferation in

Performance of FCH PET/CT in the Detection of Malignant LNs

LN Diameter	Total No. of Findings	No. of True-Positive Findings	No. of True-Negative Findings	No. of False-Negative Findings	No. of False-Positive Findings	Sensitivity (%)	Specificity (%)	Positive Predictive Value (%)	Negative Predictive Value (%)
≥5.0 mm	130	18	99	9	4	66	96	82	92
Overall	130	18	86	22	4	45	96	82	83

Note. —Overall refers to all malignant LNs, including micrometastases.

Figure 2

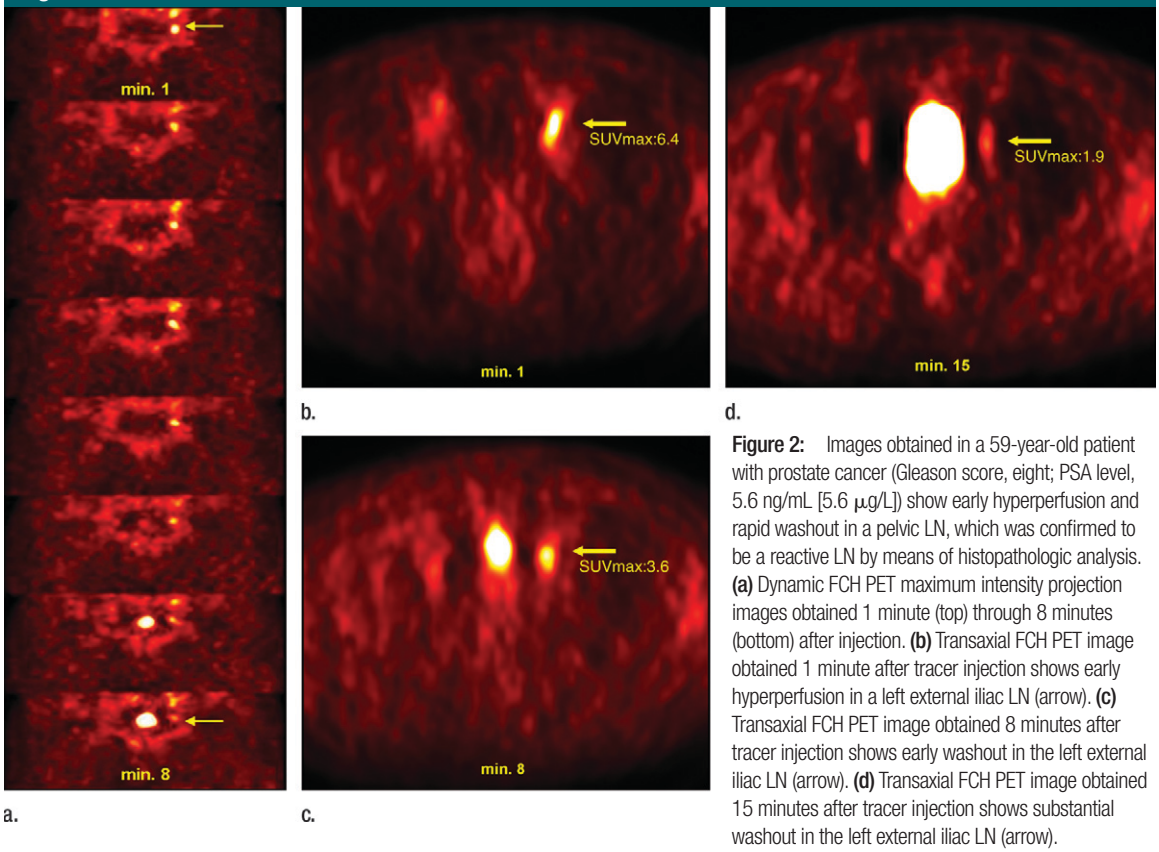

Figure 2: Images obtained in a 59-year-old patient with prostate cancer (Gleason score, eight; PSA level, 5.6 ng/mL [5.6 μg/L]) show early hyperperfusion and rapid washout in a pelvic LN, which was confirmed to be a reactive LN by means of histopathologic analysis. **(a)** Dynamic FCH PET maximum intensity projection images obtained 1 minute (top) through 8 minutes (bottom) after injection. **(b)** Transaxial FCH PET image obtained 1 minute after tracer injection shows early hyperperfusion in a left external iliac LN (arrow). **(c)** Transaxial FCH PET image obtained 8 minutes after tracer injection shows early washout in the left external iliac LN (arrow). **(d)** Transaxial FCH PET image obtained 15 minutes after tracer injection shows substantial washout in the left external iliac LN (arrow).

patients with prostate cancer, as malignancies are commonly characterized by increased proliferative activity. The second explanation is upregulation of choline kinase in cancer cells. Overexpression of choline kinase has been found in cancer cell lines, including human-derived prostate cancer (25).

In our study, we assessed the value of FCH PET/CT imaging in the preoperative staging of intermediate- and high-risk patients with prostate cancer. In the evaluation of the local tumor stage and localization of the tumor within the prostate, our results showed good agreement (81%) between regions with maximum FCH uptake on PET/CT images and sextants with maximum tumoral involvement at histopathologic analysis. However, the limitations observed by Schmid et al (15) in a similar study for initial tumor staging were also apparent in our study. Differentiation between prostate cancer and prostatitis was not possible, as intensive FCH accumulation was also seen in two patients with prostatitis. In addition, an assessment of capsular infiltration was not possible due to the limited spatial resolution of PET.

In prior studies, the value of PET imaging with radiolabeled choline in the primary assessment of LN metastases (N stage) ranged from encouraging (26) to limited (16,18,27) usefulness. De Jong et al (26) obtained promising results with ^{11}C choline PET in the preoperative LN staging of 67 patients with newly diagnosed prostate cancer, with a sensitivity of 80% in patient-based analysis. However, it should be mentioned that a mean PSA level of 123 ng/mL

Figure 3

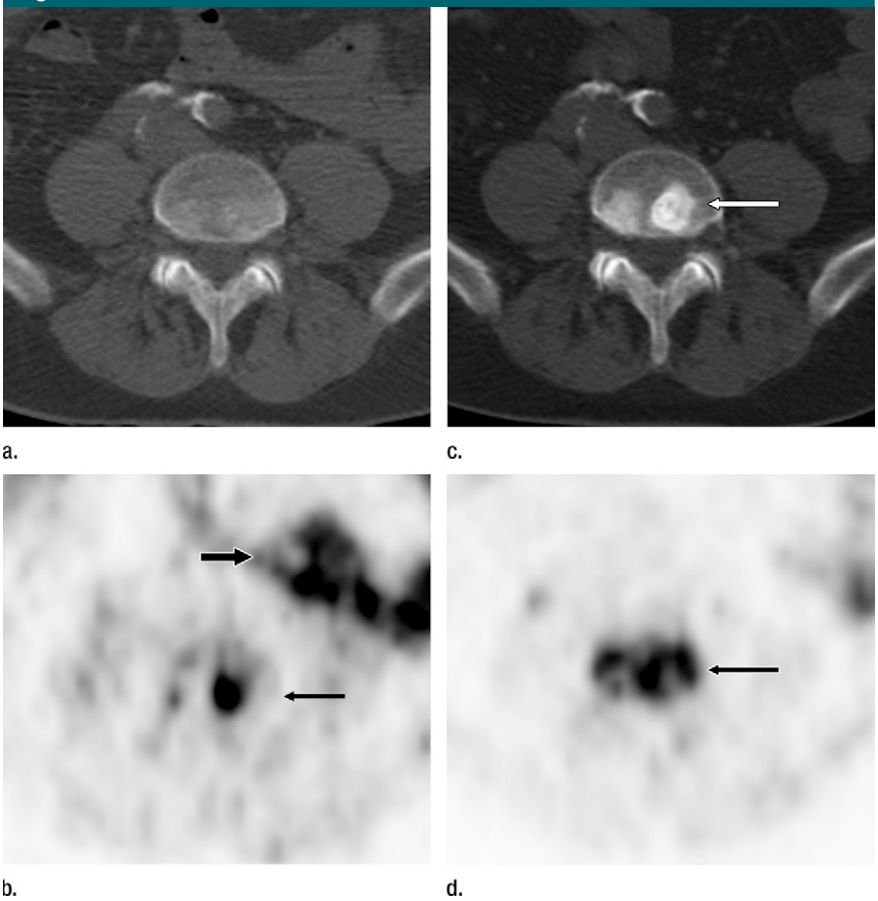

Figure 3: Images obtained in a 73-year-old patient with prostate cancer (Gleason score, seven; PSA level, 5.6 ng/mL [5.6 μg/L]) with clinical evidence of disease progression 4 months after radiation therapy and with an increase in PSA level from 0.25 ng/mL [0.25 μg/L] to 3.8 ng/mL [3.8 μg/L]. **(a)** The CT portion of an FCH PET/CT image obtained at the L4 vertebra level shows no substantial morphologic change concerning bone metastasis. **(b)** FCH PET image shows abnormal focal increased tracer uptake (long arrow) at the L4 vertebra level, probably because of bone marrow metastasis, as well as nonspecific bowel tracer uptake (short arrow). **(c)** The CT portion of an FCH PET/CT image obtained at 6-month follow-up enabled us to confirm the bone metastasis at the L4 vertebra level (arrow). **(d)** FCH PET image obtained at 6-month follow-up shows hyperactive metastatic bone lesions (arrow) at the L4 vertebra level.

(123 μg/L) may constitute a referral bias in this study. Hacker et al (18) reported that FCH PET/CT had a lower sensitivity (10%) than did sentinel node dissection (80%) in 20 patients with intermediate- or high-risk of extraglandular disease, and they concluded that FCH PET/CT was not useful in the detection of occult LN metastases. It must be noted that the mean diameter of metastatic LNs in the aforementioned study was 3.8 mm, which was less than the spatial resolution of the PET scanner (18).

In our study, FCH PET/CT showed overall sensitivity of 45%, specificity of 96%, positive predictive value of 82%, and negative predictive value of 83% in the detection of LN metastases. In LNs 5 mm in diameter or larger, the sensitivity, specificity, and positive and negative predictive values were 66%, 96%, 82%, and 92%, respectively. As expected, FCH PET/CT showed limited value in the detection of micrometastases and LN metastases smaller than 5 mm in diameter. The failure to detect small metastases in the LNs could have been caused by the limited spatial resolution of the current generation of PET scanners, which is about 4.8 mm (27,28). Although our results seem unsatisfactory for the primary node staging of patients with prostate cancer, it is important to mention that other modalities (CT, MR imaging, US) and clinical-staging nomography have limited diagnostic performance for node staging (3,4,16,29–33).

In the assessment of bone metastases, our results enabled us to confirm our previous findings (34–36) and showed that FCH PET/CT is able to depict bone metastases and has the potential to enable detection of early bone marrow infiltration.

In clinical staging, FCH PET/CT led to a change in the therapeutic care of 15% of the patient population (19 of 130 patients). When considering the entire high-risk group, 20% of the patient population (17 of 83 patients) had findings that were upstaged after FCH PET/CT, which suggests a useful clinical indication for referring patients with prostate cancer to undergo metabolic PET/CT imaging procedures.

In addition, we assessed whether dynamic (1–8 minutes after injection) or late (90 minutes after injection) imaging affect the specificity of FCH PET. One of the important findings in this study was the early FCH washout of the false-positive LNs during dynamic imaging, which might be of great concern in the differentiation of malignant versus benign LNs. Nevertheless, further research is warranted due to a small number of false-positive LNs in our study.

The limitation of this study was the lack of histologic verification for detected LNs with FCH PET/CT in 19 (15%) patients and for metastatic bone lesions in 13 (10%) patients.

In conclusion, our results suggest that FCH PET/CT can be useful as a one-stop diagnostic procedure, especially in the evaluation of high-risk patients with prostate cancer to exclude distant metastases when surgical treatment is scheduled. This modality changed the therapeutic care of 20% of high-risk patients, which suggests an

Figure 4

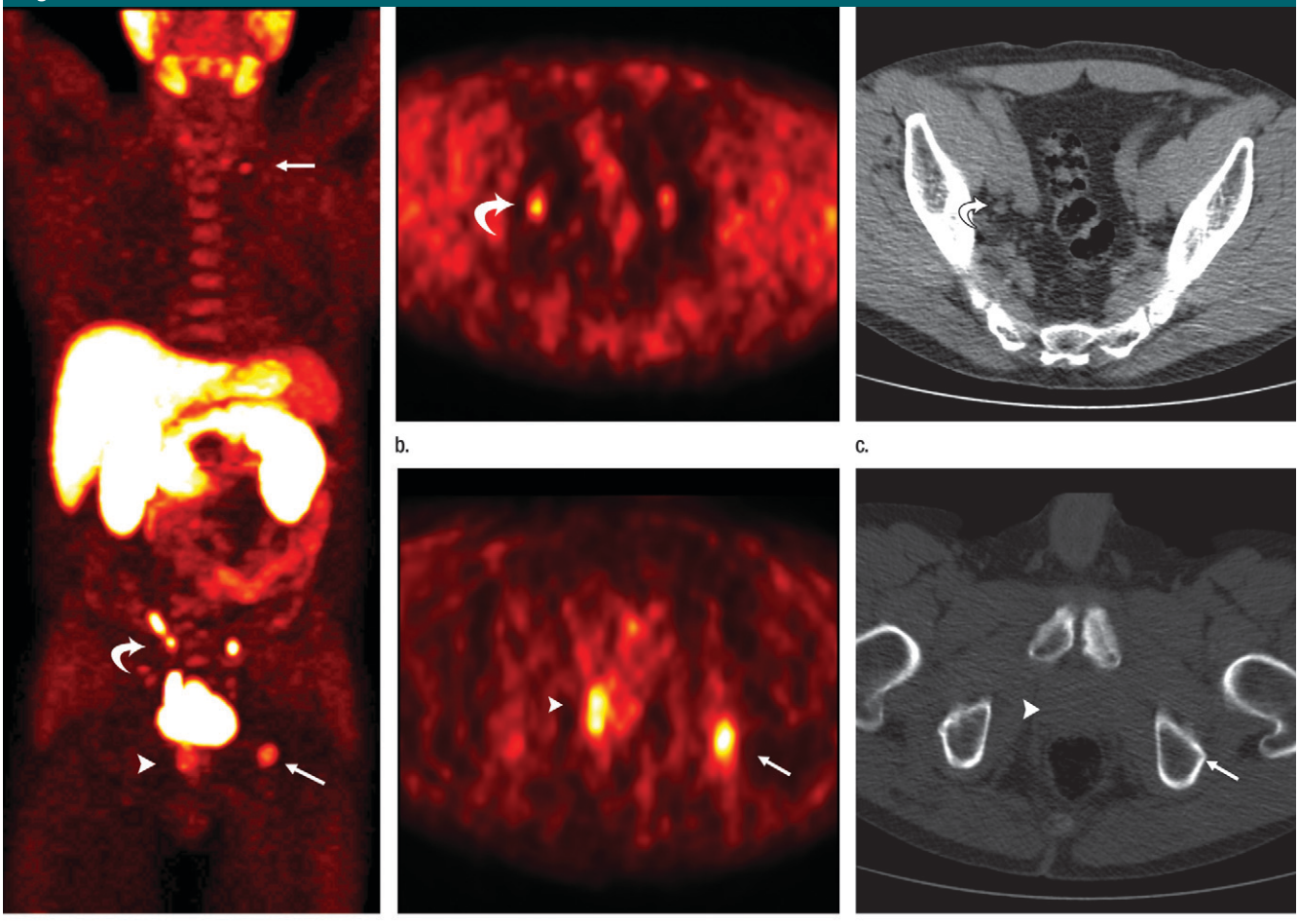

Figure 4: Images obtained in a 71-year-old patient with prostate cancer that was upstaged at FCH PET (Gleason score, seven; PSA level, 4.7 ng/mL [4.7 μg/L]). All abnormal lesions were confirmed to be malignant on the FCH PET/CT images obtained 9 months after primary staging. **(a)** Maximum intensity projection FCH PET image shows positive FCH uptake in the prostate (arrowhead), a right pelvic LN (curved arrow), and two bone metastases (straight arrows). **(b)** FCH PET image shows positive FCH uptake in a right external iliac LN metastasis (curved arrow). **(c)** The positive right pelvic LN seems to be unremarkable on the CT portion of an FCH PET/CT image, with a 9-mm short-axis diameter (arrow). **(d)** FCH PET image shows positive FCH uptake in the right lobe of the prostate (arrowhead) and in the left acetabulum (arrow). **(e)** CT portion of an FCH PET/CT image shows no substantial morphologic change in the detected lesion in the left acetabulum (arrow), probably because of early bone marrow infiltration. The lesion detected at FCH PET was localized in the right prostate lobe (arrowhead).

appropriate clinical indication for referring patients with prostate cancer to metabolic PET/CT procedures. Further studies are needed to evaluate the cost effectiveness and relative radiation dose of other imaging modalities compared with PET/CT in the preoperative evaluation of high-risk patients with prostate cancer.

References

1. Jemal A, Murray T, Ward E, et al. Cancer statistics, 2005. CA Cancer J Clin 2005; 55(1):10–30.
2. Hricak H, Schöder H, Pucar D, et al. Advances in imaging in the postoperative patient with a rising prostate-specific antigen level. Semin Oncol 2003;30(5):616–634.
3. Abuzallouf S, Dayes I, Lukka H. Baseline staging of newly diagnosed prostate cancer: a summary of the literature. J Urol 2004;171(6 pt 1):2122–2127.
4. Hricak H, Choyke PL, Eberhardt SC, Leibel SA, Scardino PT. Imaging prostate cancer: a multidisciplinary perspective. Radiology 2007;243(1):28–53.
5. Effert PJ, Bares R, Handt S, Wolff JM, Büll U, Jakse G. Metabolic imaging of untreated prostate cancer by positron emission tomography with 18fluorine-labeled deoxyglucose. J Urol 1996;155(3):994–998.
6. Heicappell R, Müller-Mattheis V, Reinhardt M, et al. Staging of pelvic lymph nodes in neoplasms of the bladder and prostate by positron emission tomography with 2-[(18)F]-2-deoxy-D-glucose. Eur Urol 1999; 36(6):582–587.
7. Hofer C, Laubenbacher C, Block T, Breul J, Hartung R, Schwaiger M. Fluorine-18-fluorodeoxyglucose positron emission tomography is useless for the detection of local recurrence after radical prostatectomy. Eur Urol 1999;36(1):31–35.

8. Liu IJ, Zafar MB, Lai YH, Segall GM, Terris MK. Fluorodeoxyglucose positron emission tomography studies in diagnosis and staging of clinically organ-confined prostate cancer. Urology 2001;57(1):108–111.
9. Morris MJ, Akhurst T, Osman I, et al. Fluorinated deoxyglucose positron emission tomography imaging in progressive metastatic prostate cancer. Urology 2002; 59(6):913–918.
10. Shreve PD, Grossman HB, Gross MD, Wahl RL. Metastatic prostate cancer: initial findings of PET with 2-deoxy-2-[F-18]fluoro-D-glucose. Radiology 1996;199(3):751–756.
11. Langsteger W, Heinisch M, Fogelman I. The role of fluorodeoxyglucose, 18F-dihydroxyphenylalanine, 18F-choline, and 18F-fluoride in bone imaging with emphasis on prostate and breast. Semin Nucl Med 2006;36(1):73–92.
12. Cimitan M, Bortolus R, Morassut S, et al. [18F]fluorocholine PET/CT imaging for the detection of recurrent prostate cancer at PSA relapse: experience in 100 consecutive patients. Eur J Nucl Med Mol Imaging 2006;33(12):1387–1398.
13. Reske SN, Blumstein NM, Neumaier B, et al. Imaging prostate cancer with 11C-choline PET/CT. J Nucl Med 2006;47(8): 1249–1254.
14. Kwee SA, Wei H, Sesterhenn I, Yun D, Coel MN. Localization of primary prostate cancer with dual-phase 18F-fluorocholine PET. J Nucl Med 2006;47(2):262–269.
15. Schmid DT, John H, Zweifel R, et al. Fluorocholine PET/CT in patients with prostate cancer: initial experience. Radiology 2005;235(2):623–628.
16. Schiavina R, Scattoni V, Castellucci P, et al. 11C-choline positron emission tomography/computerized tomography for preoperative lymph-node staging in intermediate-risk and high-risk prostate cancer: comparison with clinical staging nomograms. Eur Urol 2008;54(2):392–401.
17. Testa C, Schiavina R, Lodi R, et al. Prostate cancer: sextant localization with MR imaging, MR spectroscopy, and 11C-choline PET/CT. Radiology 2007;244(3):797–806.
18. Häcker A, Jeschke S, Leeb K, et al. Detection of pelvic lymph node metastases in patients with clinically localized prostate cancer: comparison of [18F]fluorocholine positron emission tomography-computerized tomography and laparoscopic radioisotope guided sentinel lymph node dissection. J Urol 2006;176(5):2014–2018; discussion 2018–2019.
19. Scher B, Seitz M, Albinger W, et al. Value of 11C-choline PET and PET/CT in patients with suspected prostate cancer. Eur J Nucl Med Mol Imaging 2007;34(1): 45–53.
20. Goldstein NS, Bégin LR, Grody WW, Novak JM, Qian J, Bostwick DG. Minimal or no cancer in radical prostatectomy specimens: report of 13 cases of the "vanishing cancer phenomenon". Am J Surg Pathol 1995;19(9):1002–1009.
21. Vassiliev D, Krasikova R, Kutznetsova O, Federova O, Nader M. Simple HPLC method for the detection of N,N-dimethylaminoethanol in the preparation of [N-methyl-11C] choline. Eur J Nucl Med Mol Imaging 2003; 30(suppl):342P.
22. Schröder FH, Roach M 3rd, Scardino P. Clinical decisions: management of prostate cancer. N Engl J Med 2008;359(24): 2605–2609.
23. Harisinghani MG, Barentsz J, Hahn PF, et al. Noninvasive detection of clinically occult lymph-node metastases in prostate cancer. N Engl J Med 2003;348(25):2491–2499.
24. Breeuwsma AJ, Pruim J, Jongen MM, et al. In vivo uptake of [11C]choline does not correlate with cell proliferation in human prostate cancer. Eur J Nucl Med Mol Imaging 2005;32(6):668–673.
25. Zheng QH, Gardner TA, Raikwar S, et al. [11C]Choline as a PET biomarker for assessment of prostate cancer tumor models. Bioorg Med Chem 2004;12(11):2887–2893.
26. de Jong IJ, Pruim J, Elsinga PH, Vaalburg W, Mensink HJ. Preoperative staging of pelvic lymph nodes in prostate cancer by 11C-choline PET. J Nucl Med 2003;44(3):331–335.
27. Husarik DB, Miralbell R, Dubs M, et al. Evaluation of [(18)F]-choline PET/CT for staging and restaging of prostate cancer. Eur J Nucl Med Mol Imaging 2008;35(2):253–263.
28. Conti M. State of the art and challenges of time-of-flight PET. Phys Med 2009;25(1):1–11.
29. Hricak H, Dooms GC, Jeffrey RB, et al. Prostatic carcinoma: staging by clinical assessment, CT, and MR imaging. Radiology 1987;162(2):331–336.
30. Platt JF, Bree RL, Schwab RE. The accuracy of CT in the staging of carcinoma of the prostate. AJR Am J Roentgenol 1987; 149(2):315–318.
31. Golimbu M, Morales P, Al-Askari S, Shulman Y. CAT scanning in staging of prostatic cancer. Urology 1981;18(3):305–308.
32. Rørvik J, Halvorsen OJ, Albrektsen G, Haukaas S. Lymphangiography combined with biopsy and computer tomography to detect lymph node metastases in localized prostate cancer. Scand J Urol Nephrol 1998;32(2):116–119.
33. Wolf JS Jr, Cher M, Dall'era M, Presti JC Jr, Hricak H, Carroll PR. The use and accuracy of cross-sectional imaging and fine needle aspiration cytology for detection of pelvic lymph node metastases before radical prostatectomy. J Urol 1995;153(3 pt 2):993–999.
34. Beheshti M, Vali R, Waldenberger P, et al. Detection of bone metastases in patients with prostate cancer by 18F fluorocholine and 18F fluoride PET-CT: a comparative study. Eur J Nucl Med Mol Imaging 2008;35(10):1766–1774.
35. Beheshti M, Vali R, Waldenberger P, et al. The use of F-18 choline PET in the assessment of bone metastases in prostate cancer: correlation with morphological changes on CT. Mol Imaging Biol 2009;11(6):446–454.
36. Beheshti M, Vali R, Langsteger W. [18F] fluorocholine PET/CT in the assessment of bone metastases in prostate cancer. Eur J Nucl Med Mol Imaging 2007;34(8):1316–1317; author reply 1318–1319.